hMSC-mediated Concurrent Delivery of Endostatin and Carboxylesterase to Mouse Xenografts Suppresses Glioma Initiation and Recurrence

Jinlong Yin[1], Jun-Kyum Kim[2], Jai-Hee Moon[2], Samuel Beck[1], Dachuan Piao[1], Xun Jin[2], Sung-Hak Kim[2], Young Chang Lim[3], Do-Hyun Nam[4], Seungkwon You[2], Hyunggee Kim[2] and Yun-Jaie Choi[1]

[1]National Research Laboratory of Animal Cell Biotechnology, School of Agricultural Biotechnology, Seoul National University, Seoul, Republic of Korea; [2]School of Life Sciences and Biotechnology, Korea University, Seoul, Republic of Korea; [3]Department of Otorhinolaryngology-Head and Neck Surgery, Research Institute of Medical Science, Konkuk University School of Medicine, Seoul, Republic of Korea; [4]Department of Neurosurgery, Samsung Medical Center and Samsung Biomedical Research Institute, Sungkyunkwan University School of Medicine, Seoul, Republic of Korea

Glioma stem cells (GSCs) are known to be maintained within a "vascular niche"; thereby, disruption of this microenvironment using antiangiogenesis agents is a promising therapeutic modality. However, this regimen leads to treatment failure and tumor recurrence in patients with glioblastoma multiforme (GBM). Therefore, more effective therapeutic approaches that can eradicate GSCs and the bulk tumors are needed. Toward this goal, we examined the antitumor effects of an antiangiogenesis approach combined with conventional chemotherapy on suppressing glioma xenograft growth. We established three genetically engineered mesenchymal stem cell (MSC) lines (GE-AF-MSCs) by stably transducing the gene encoding endostatin (an antiangiogenesis factor), the gene encoding secretable form of carboxylesterase 2 (sCE2, a prodrug-activating enzyme), or a mixture of both genes. Among the three GE-AF-MSC cell lines, injection of amniotic fluid (AF)-MSCs-endostatin-sCE2 cells into U87MG-EGFRvIII-driven orthotopic brain tumor and post-surgery tumor recurrence models, and subsequent CPT11 treatment yielded the strongest antitumor responses, including diminished angiogenesis, increased cell death, and a reduced Nestin-positive GSC population. Therefore, our antitumor strategy provides a novel basis for designing stem cell-mediated therapeutic approaches to target and eradicate GSCs and the bulk tumors.

Received 21 August 2010; accepted 1 February 2011; published online 8 March 2011. doi:10.1038/mt.2011.28

INTRODUCTION

Glioblastoma multiforme (GBM) is the most malignant and aggressive type of brain tumor. Despite considerable advances in glioma biology, GBM remains one of the most incurable malignancies, with a median survival of <1 year.[1] Recent studies have demonstrated that a sub-population of glioma cells in GBM and other types of aggressive brain tumors exhibit stem cell properties—self-renewal and multilineage differentiation—and tumor-initiating potential.[2] Thus, these cells are referred to as glioma stem cells (GSCs).[3] Clinically, GSCs are considered to be major culprits for GBM recurrence after conventional therapies such as surgical resection, chemotherapy, and/or radiotherapy,[4] because of their intrinsic resistance to chemotherapy[5] and irradiation.[6] Therefore, although current GBM therapies can significantly diminish the bulk of a tumor, they cannot completely eradicate GSCs and prevent tumor recurrence,[7] supporting the idea that GSCs are important therapeutic targets to overcome current clinical limitations in patients with GBM.

Similar to normal neural stem cells (NSCs), GSCs reside within a "vascular niche" and maintain their stemness in this microenvironment,[8] implying that disruption of the GSC vascular niche with antiangiogenesis drugs such as vascular endothelial growth factor monoclonal antibody, is a promising therapeutic modality.[9] However, in reality, this regimen eventually leads to treatment failure and tumor recurrence in patients with GBM.[10] Therefore, more effective therapeutic approaches that can eliminate both GSCs and the bulk tumor are necessary for GBM therapy.

Human mesenchymal stem cells (MSCs) are multipotent cells that can differentiate into various cell types.[11,12] Clinically, MSCs are particularly attractive because they can be easily isolated, expanded in culture, and genetically manipulated using currently available molecular techniques.[13–15] Additionally, MSCs can migrate toward glioma,[16] and recently, genetically engineered MSCs demonstrated potent antitumor effects in an *in vivo* glioma model.[17,18] Therefore, considerable improvement in understanding of the nature of MSCs may shed light on their potential as a delivery vehicle for various antitumor agents.

Endostatin, a cleavage product of collagen XVIII,[19] is a potent antiangiogenic agent that inhibits endothelial cell migration and proliferation, leading to suppression of tumor growth and progression in mice.[19,20] The carboxylesterases (CEs) can convert the prodrug CPT11, a water-soluble camptothecin derivative, into the more active lipophilic metabolite, SN-38.[21] Although patients

Correspondence: *Yun-Jaie Choi, National Research Laboratory of Animal Cell Biotechnology, School of Agricultural Biotechnology, Seoul National University, Shinlim-dong, Kwanak-gu, Seoul 151–742, Republic of Korea. E-mail: cyjcow@snu.ac.kr or Hyunggee Kim, School of Life Sciences and Biotechnology, Korea University, 5-ga, Anam-dong, Seongbuk-gu, Seoul 136–713, Republic of Korea. E-mail: hg-kim@korea.ac.kr*

express CEs, only 5–10% of CPT11 is converted into active SN-38, when systemically administered.[22] Additionally, the clinical use of CPT11 is hampered by dose-dependent toxicity, primarily causing diarrhea.[23] Therefore, a strategy that accelerates the antitumor efficacy of CPT11 without the unwanted side-effects is selectively increasing CE activity at the tumor site.[24]

To explore the potent synergistic effects of the antiangiogenesis approach combined with conventional chemotherapy in eradicating GSCs and the bulk tumors, we used human amniotic fluid (AF)-derived MSCs[25] as the delivery vehicle for an endostatin and a secretable form of carboxylesterase 2 (sCE2) to glioma xenografts. Here, we show that delivery of endostatin and sCE2 by MSCs at the tumor sites along with CPT11 treatment exhibits reliable antitumor effects in U87MG-EGFRvIII-driven orthotopic brain tumor and postsurgery tumor recurrence models.

RESULTS

U87MG-endostatin cells suppress *in vitro* tube formation of endothelial cells, and tumor growth and angiogenesis in their xenograft tumors

To explore the potent effect of endostatin in tumor angiogenesis, we first established an endostatin-overexpressing U87MG (U87MG-endostatin) and control U87MG (U87MG-hygro) cell lines by transfection of pSecTag2/Endostatin/HygroB vector and pSecTaq2/HygroB empty vector, respectively. Endostatin overexpression did not influence proliferation in these cells at day 3, but slightly increased their growth at day 5 (**Figure 1a**). However, the *in vitro* tube-forming ability of human umbilical vein endothelial cells (HUVECs) was significantly suppressed when grown in U87MG-endostatin-derived conditioned media (CM) supplemented with or without vascular endothelial growth factor, compared with endothelial differentiation medium and U87MG-hygro-derived CM (**Figure 1b** and **Supplementary Figure S1**), supporting a previous idea that endostatin is a potent antiangiogenesis factor that inhibits vascular endothelial cell differentiation.[26]

To investigate the *in vivo* effect of endostatin on tumor growth, we subcutaneously injected U87MG-endostatin and U87MG-hygro cells into nude mice. Endostatin overexpression significantly reduced tumor growth (**Figure 1c**) and volume (**Figure 1d**), compared with that of U87MG-hygro cells. In addition, microvessel formation in tumors arising from U87MG-endostatin cells markedly decreased as observed by reduced $CD31^+$ endothelial cells and vessel shapes (**Figure 1e** and **Supplementary Figure S2**), indicating that endostatin can inhibit the tumorigenic potential of glioma cells by suppressing angiogenesis *in vivo*.

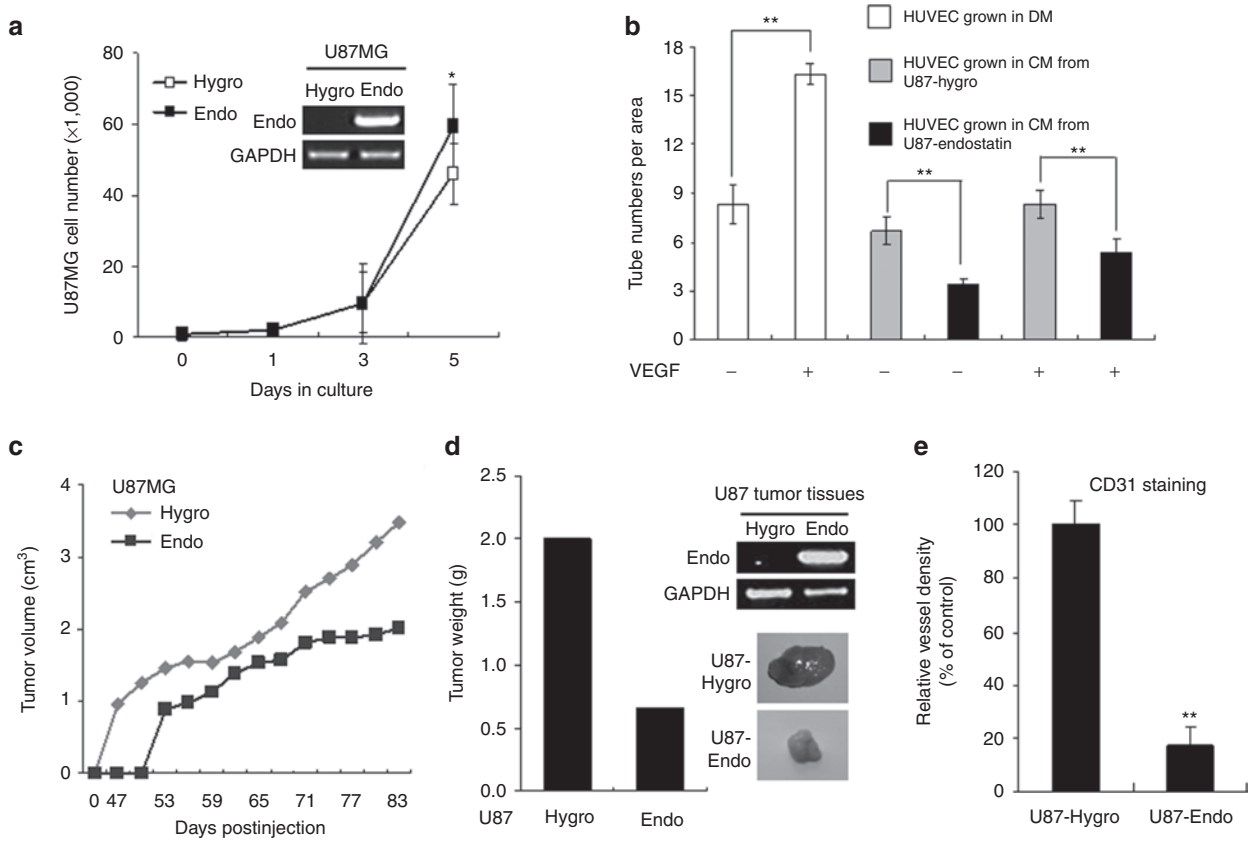

Figure 1 Endostatin overexpression in U87MG cells inhibits *in vitro* tube formation of human umbilical vein endothelial cells (HUVECs) and *in vivo* tumor growth and angiogenesis. (**a**) *In vitro* growth rate of U87MG-endostatin and control U87MG-hygro cells. Expression levels of endostatin in these cells were determined by semiquantitative real-time reverse transcription-PCR (RT-PCR; inset). *$P < 0.05$. (**b**) *In vitro* tube formation of HUVECs was suppressed when grown in U87MG-endostatin-derived conditioned media (CM) in the presence or absence of vascular endothelial growth factor (VEGF). **$P < 0.01$. (**c**) Endostatin overexpression in U87MG cells decreased *in vivo* subcutaneous tumor growth. (**d**) Tumor weight (left panel), representative photos showing tumors (right low panel), and endostatin mRNA levels (right upper panel) in tumors derived from the subcutaneous injection of U87MG-hygro and U87MG-endostatin cells. (**e**) Endostatin overexpression in U87MG cells reduced vessel formation in xenograft tumors. **$P < 0.01$.

sCE2 confers enhanced cytotoxic efficacy of CPT11 to glioma cells

Next, U87MG cells were transduced with a secretable form of sCE2 that converts the prodrug CPT11 to the active lipophilic metabolite SB-38 (**Figure 2a**, inset). We then performed an MTT [3-(4,5-dimethylthiazol-2-yl)-2,5-diphenyltetrazolium bromide] assay to determine whether sCE2 overexpression could influence cell viability, and found that sCE2 did not decrease cell viability, but instead slightly increased cell survival (**Figure 2a**). However, after treatment with CPT11, U87MG-sCE2 cells exhibited a significant reduction in cell viability as determined by Annexin V/PI-mediated fluorescence-activated cell sorting analysis (**Figure 2b**). Additionally, U87MG-EGFRvIII cells (containing a constitutively active epidermal growth factor receptor mutant[27]) showed a marked decrease in their viability when grown in U87MG-sCE2-derived CM combined with CPT11 compared with control cells (**Figure 2c**). Together, our findings demonstrate that a secretable carboxylesterase (sCE) confers enhanced cytotoxic efficacy of CPT11 to glioma cells, presumably due to the accumulation of active SB-38.

Three GE-AF-MSC cell lines possess the traits of MSCs

Based on our findings that demonstrate the potent antitumor effects of both endostatin and sCE2 in U87MG cells *in vivo* and *in vitro*, we used human AF-MSCs as a vehicle for the specific delivery of endostatin and sCE2 into the tumors, because of its homing properties in tumors.[18] Thus, we overexpressed the gene encoding endostatin, the gene encoding sCE2, and both genes into AF-MSCs, thereby establishing three genetically engineered AF-MSC cell lines (GE-AF-MSCs; **Supplementary Figure S3**). We then investigated whether these three GE-AF-MSC cell lines maintained their fundamental MSC nature by analyzing their MSC marker expression and differentiation potential to adipogenic and osteogenic cell lineages along with differentiated cell marker expression. IF-FACS analysis revealed that all three GE-AF-MSC cell lines, along with control AF-MSCs-hygro, express typical MSC marker proteins such as CD13, CD29, and CD44,[28,29] but not CD31 (an endothelial marker), CD34 (a primitive hematopoietic marker), CD45 (a mature hematopoietic marker), and CD133 (a NSC marker; **Supplementary Figure S4a**). Furthermore, when cultured in adipogenic or osteogenic differentiation medium, the three GE-AF-MSC cell lines could differentiate into adipocytes

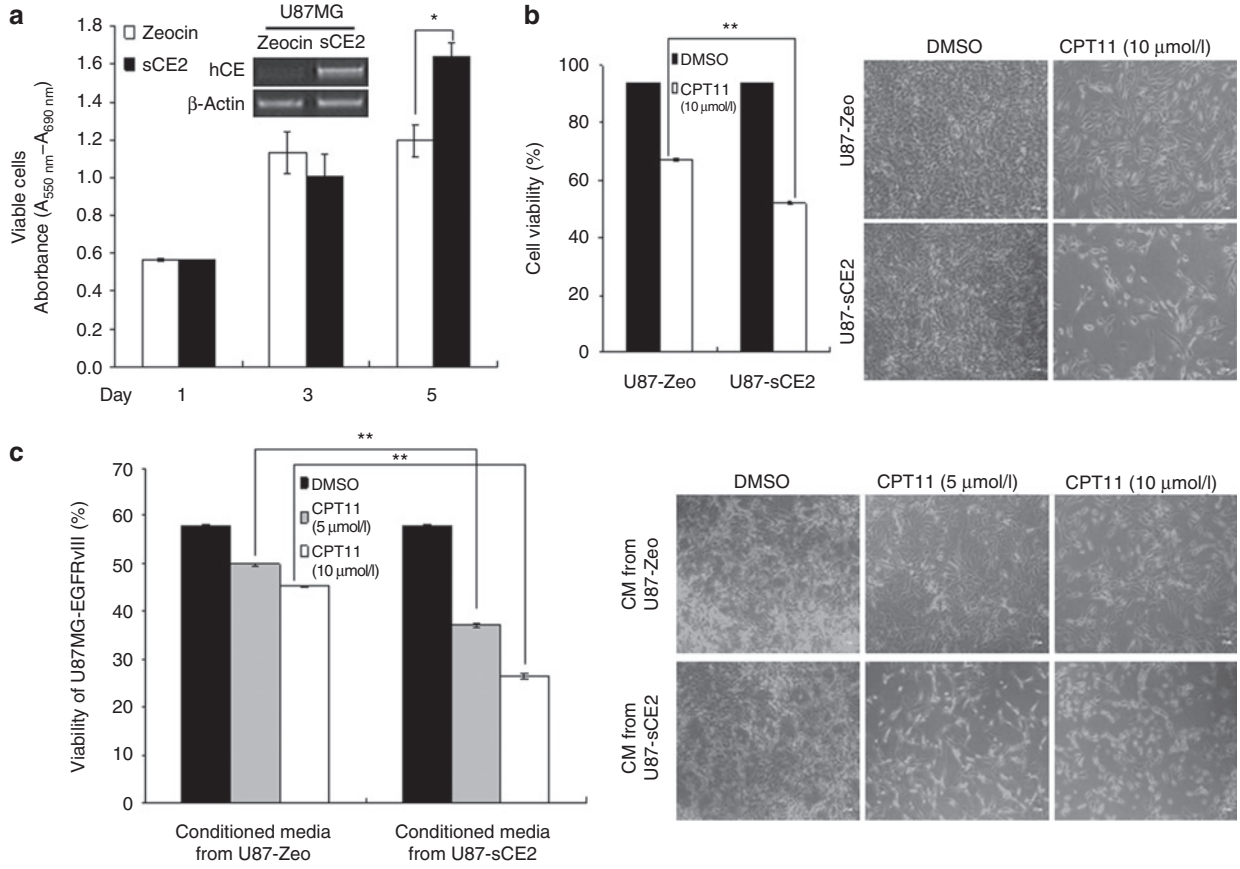

Figure 2 Secretable form of carboxylesterase 2 (sCE2) overexpression in U87MG cells decreases cell viability after CPT11 treatment. (**a**) Cell viability of U87MG-sCE2 and U87MG-control cells were determined by the MTT [3-(4,5-dimethylthiazol-2-yl)-2,5-diphenyltetrazolium bromide] assay. Expression levels of sCE2 in these cells were determined by real-time reverse transcription-PCR (RT-PCR) (inset). *$P < 0.05$. (**b**) Cell viability (left) of U87MG-sCE2 and control U87MG-Zeo cells treated with or without CPT11 was determined by Annexin V/propidium iodide (PI)-mediated fluorescence-activated cell sorting (FACS) analysis. Representative photos (right) showing U87MG-sCE2 and U87MG-control cells grown in the above experimental setting. **$P < 0.01$. (**c**) Cell viability (left) of U87MG-EGFRvIII cells grown in U87MG-sCE2-derived conditioned media (CM) in the presence of different concentrations of CPT11 (0, 5, and 10 μmol/l) was determined by Annexin V/PI-mediated FACS analysis. Representative photos (right) showing U87MG-EGFRvIII cells grown in the above experimental setting. **$P < 0.01$.

or osteoblasts [**Supplementary Figure S4b** (ref. 29)], and express the adipogenic genes *aP2* and *PPARγ2* or the osteogenic genes *osteopontin* and *osteocalcin* (**Supplementary Figure S4c**). We also performed a migration assay using a transwell chamber to evaluate the migratory property of AF-MSCs labeled with a membrane-permeable CSR dye. As shown in **Figure 3a**, AF-MSCs increased their migration to the highly aggressive glioma cell lines U87MG-EGFRvIII and U87MG-ID3 cells (X. Jin, J. Yin, S.H. Kim, Y.W. Sohn, S. Beck, T.C. Kang *et al.*, unpublished results) compared with normal human astrocytes and parental U87MG cells. Together, these data indicate that our genetically engineered AF-MSCs retain their MSC traits.

The antitumor effects of GE-AF-MSCs on HUVECs and glioma cells *in vitro*, as well as primary brain tumor growth *in vivo*

In agreement with antiangiogenesis and the antitumor effects of U87MG-endostatin and U87MG-sCE2, respectively (**Figures 1** and **2**), the *in vitro* tube formation of HUVECs was significantly inhibited when grown in AF-MSCs-endostatin-derived CM (**Figure 3b**), whereas the cytotoxicity of U87MG-EGFRvIII to CPT11 increased when grown in AF-MSCs-sCE2-derived CM (**Figure 3c**). EGFRvIII overexpression allows U87MG to acquire GSC features such as self-renewal, aberrant differentiation, and heterogeneous tumor formation (X. Jin, J. Yin, S.H. Kim, Y.W. Sohn, S. Beck, T.C. Kang *et al.*, unpublished results).[30] A mixture of U87MG-EGFRvIII labeled with NIR797 fluorescence dye and each GE-AF-MSC line was orthotopically injected in the nude mice to assess the antitumor effects of endostatin and sCE2 on gliomagenesis *in vivo*. As orthotopically injected into nude mouse brains, GE-AF-MSCs with or without CPT11 treatment did not give rise to tumor formation and negligible apoptotic cell death as determined by hematoxylin & eosin and cleaved caspase 3 staining, respectively (**Supplementary Figure S5a**). Furthermore, all mice used in *in vivo* studies displayed normal behaviors and body weights without potential toxicities during experimental period. Serum chemistry data showed no significant differences in albumin and total bilirubin levels. Although there was a slight change in levels of alanine aminotransferase, aspartate aminotransferase, and blood urea nitrogen, all mice were shown to maintain serum protein and liver enzymes levels in the normal physiological ranges (**Supplementary Figure S5b**).

Whole-body fluorescence imaging of mice orthotopically implanted with a mix of NIR797-labeled U87MG-EGFRvIII and GE-AF-MSCs (5:1 ratio) and treated with CPT11 revealed a significant reduction in tumor burden in mice-bearing AF-MSCs-endostatin or AF-MSCs-sCE2. However, the most potent antitumor effect was observed in tumors simultaneously implanted with AF-MSCs-endostatin-sCE2 at day 17 postinjection (**Figure 4a**), and was further confirmed by analyzing fluorescence signals in the extracted brains and staining brain sections with hematoxylin & eosin (**Supplementary Figure S6** and **Figure 4b**). Notably, the antitumor effects observed in our experimental setting were achieved using a relatively lower amount of CPT11 (0.5 mg) compared with that used in previous studies.[31]

As shown in **Figure 4b**, compared with AF-MSCs-hygro, immunohistochemistry (IHC) assays of brain sections revealed the following: the vessel density ($CD31^+$) was markedly decreased by AF-MSCs-endostatin and AF-MSCs-endostatin-sCE2; the cell proliferation rate ($Ki67^+$) was suppressed by AF-MSCs-sCE2 and AF-MSCs-endostatin-sCE2; the apoptotic index (active cleaved caspase 3^+) was markedly elevated by all three GE-AF-MSC cell lines; and the GSC population ($Nestin^+$) was dramatically reduced by AF-MSCs-endostatin and AF-MSCs-endostatin-sCE2. Conversely, differentiated cells ($GFAP^+$ and $S100\beta^+$) were markedly increased by AF-MSCs-endostatin and AF-MSCs-endostatin-sCE2 (**Figure 4b**). Together, although delivery of the genes encoding endostatin or sCE2 into the tumors exerted a partial antitumor effect, the combined delivery of these genes caused the extensive eradication of GSCs and the bulk of tumors.

The antitumor effects of the simultaneous delivery of endostatin and sCE2 by AF-MSCs in a postsurgery tumor recurrence model

To assess the antitumor effects of GE-AF-MSCs in tumor recurrence after surgical resection, we first created subcutaneous

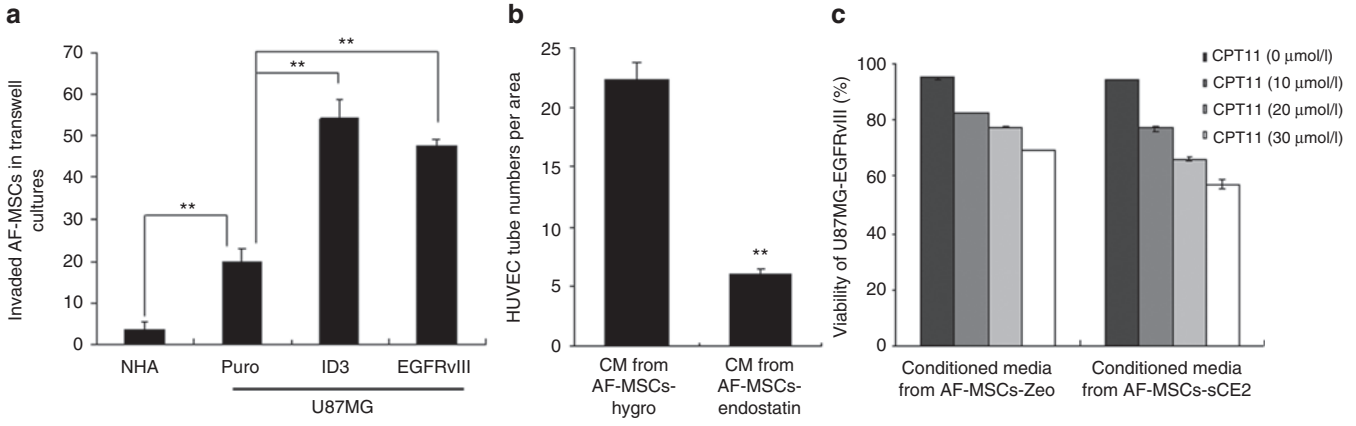

Figure 3 *In vitro* **migration of amniotic fluid-derived mesenchymal stem cells (AF-MSCs) and the effects of GE-AF-MSCs on** *in vitro* **tube formation of human umbilical vein endothelial cells (HUVECs) and glioma cell viability.** (**a**) Increased CSR-labeled AF-MSC migration to highly aggressive glioma cells such as U87MG-EGFRvIII and U87MG-ID3 cells. $^{**}P < 0.01$. (**b**) *In vitro* tube formation of HUVECs grown in AF-MSCs-endostatin-derived conditioned media (CM). $^{**}P < 0.01$. (**c**) Cell viability of U87MG-EGFRvIII grown in AF-MSCs-sCE2-derived CM with or without CPT11 treatment was determined by Annexin V/PI-mediated fluorescence-activated cell sorting (FACS) analysis. There was a significant difference in viability of U87MG-EGFRvIII cells grown in the AF-MSCs-Zeo-derived CM and AF-MSCs-sCE2-derived CM in the presence of CPT11. $P < 0.01$.

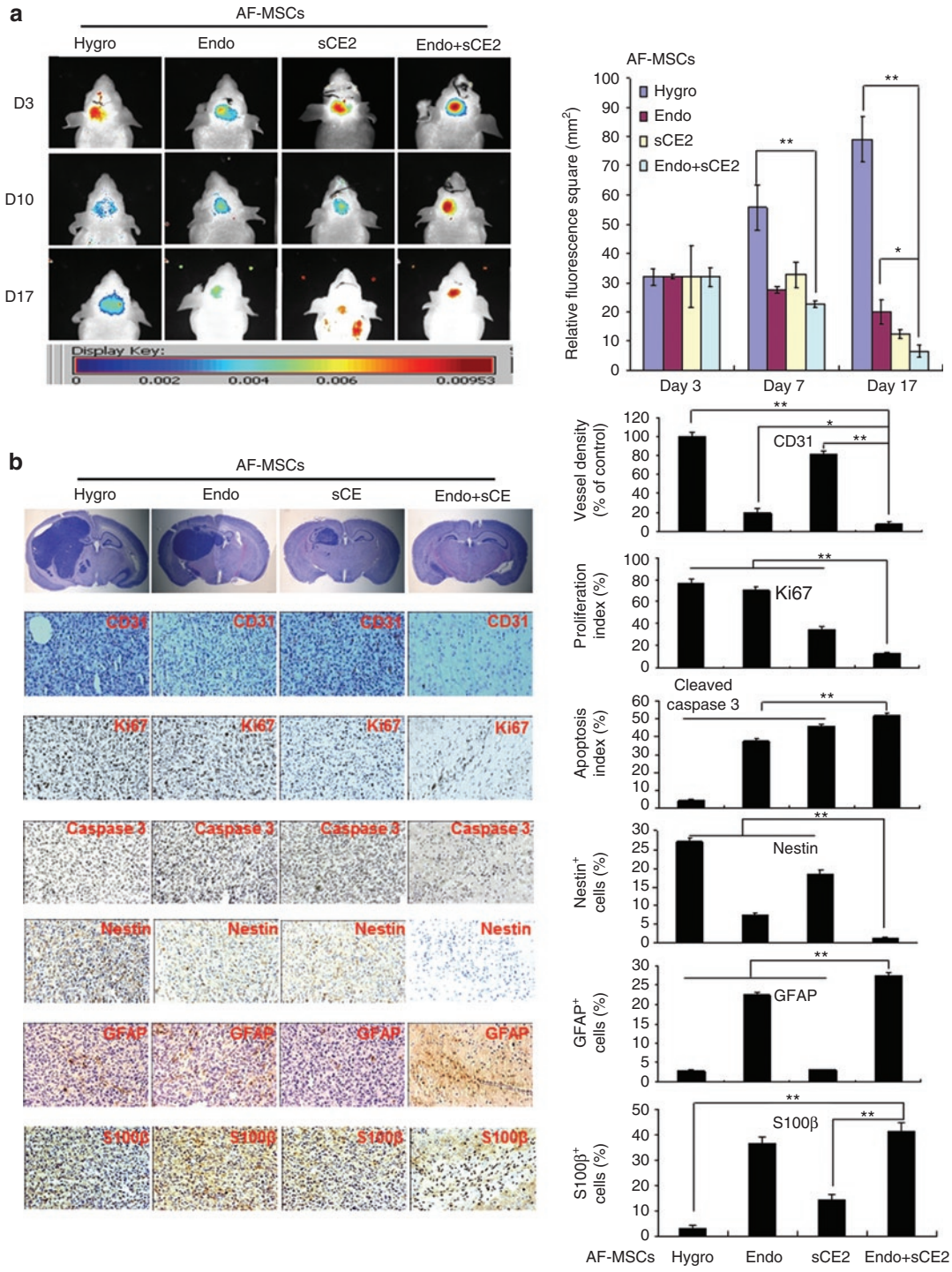

Figure 4 Antitumor effects of genetically engineered amniotic fluid-derived mesenchymal stem cells (GE-AF-MSCs) on primary brain tumor growth *in vivo*. (**a**) Whole-body fluorescence images (left panel) showing tumors derived from the simultaneous implantation of NIR797-labeled U87MG-EGFRvIII and AF-MSCs-hygro or three GE-AF-MSC cell lines were collected at different time periods (day 3, 10, and 17 postimplantation). Quantitative data of fluorescence signals are shown in the right panel. *$P < 0.05$ and **$P < 0.01$. (**b**) Mice were sacrificed 17 days after injection. Hematoxylin & eosin (H&E) staining and immunohistochemistry (IHC) images (left panel) of tumors derived from the simultaneous implantation of U87MG-EGFRvIII and AF-MSCs-hygro or three GE-AF-MSC cell lines stained with CD31, Ki67, cleaved caspase 3, Nestin, and glial fibrillary acidic protein (GFAP) antibodies. The right panel shows quantitative data of IHC analysis. *$P < 0.05$ and **$P < 0.01$.

tumors by injecting U87MG-EGFRvIII cells into nude mice. As tumor sizes reached 1.8–2.2 cm^3, ~90% of the tumor mass was surgically removed, and then the three GE-AF-MSC cell lines and AF-MSCs-hygro were implanted in the resection cavity of the tumors (see Materials and Methods section). Compared with AF-MSCs-hygro and other GE-AF-MSCs tested, AF-MSCs-endostatin-sCE2 showed the most significant suppression of tumor regrowth in the presence of CPT11 as examined by the

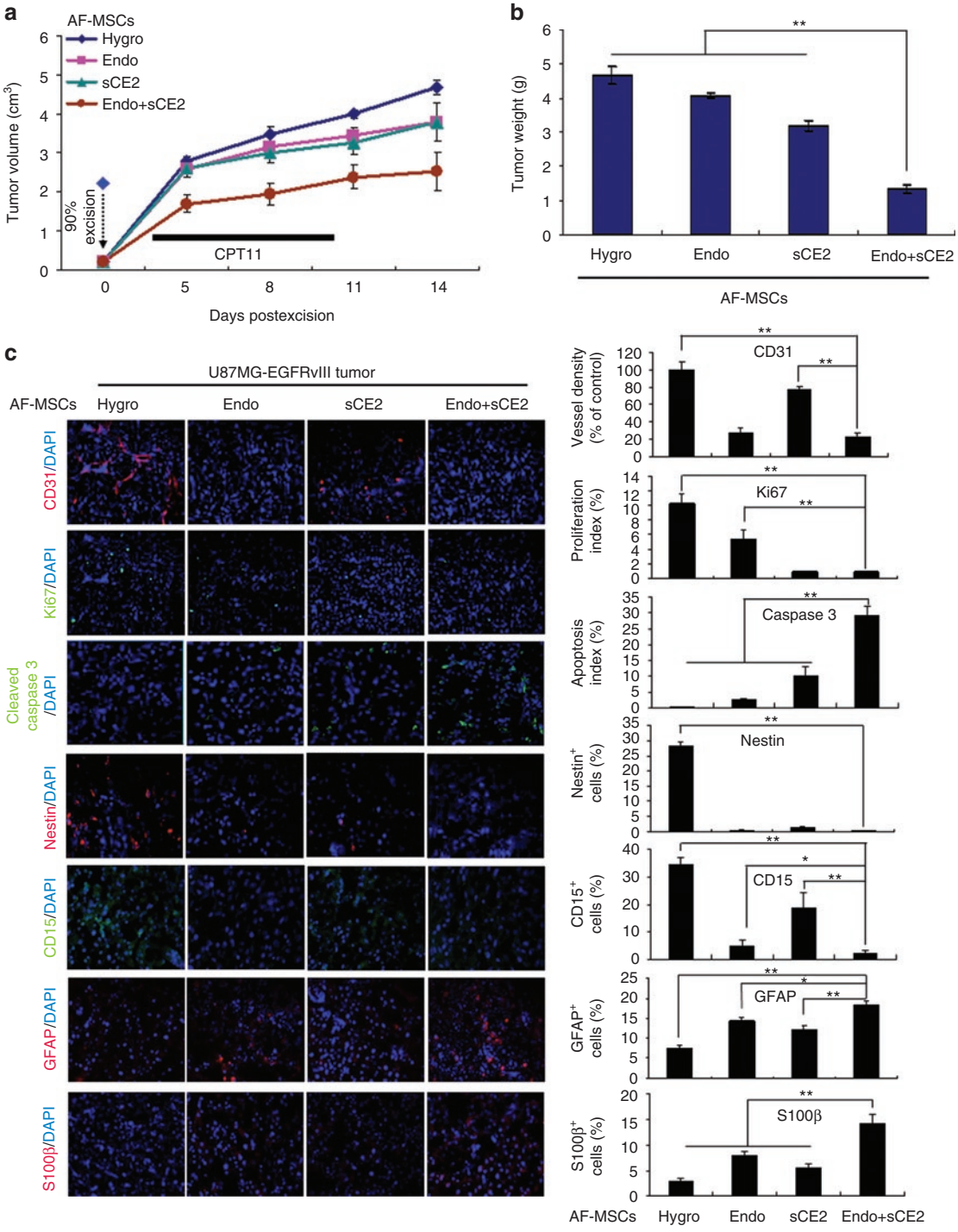

Figure 5 Antitumor effects of genetically engineered amniotic fluid-derived mesenchymal stem cells (GE-AF-MSCs) in a postsurgery tumor recurrence model. (**a**,**b**) The AF-MSCs-hygro or each GE-AF-MSC cell line was implanted into the resection cavity of U87MG-EGFRvIII-driven tumors in which ~90% of the tumor mass had been surgically removed. The antitumor effects of GE-AF-MSCs and CPT11 treatment in this tumor recurrence model were investigated by measuring the (**a**) tumor growth rate and (**b**) tumor volume. $^{**}P < 0.01$. (**c**) Immunofluorescence (IF) images (left panel) of recurrent tumors stained with CD31, Ki67, cleaved caspase 3, Nestin, and GFAP antibodies. 4′,6-diamidino-2-phenylindole (DAPI; blue) was used for nuclear staining. The right panel shows quantitative data of immunofluorescence (IF) analysis. $^{*}P < 0.05$ and $^{**}P < 0.01$.

tumor growth rate (Figure 5a) and volume (Figure 5b). Notably, the fluorescence signals attained from AF-MSCs-sCE2 cells labeled with NIR730 dye were detected in the tumor masses throughout the experiment period (**Supplementary Figure S7a,b**), implying that GE-AF-MSCs are relatively resistant to CPT11.

As shown in Figure 5c, compared with AF-MSCs-hygro, our immunofluorescence (IF) assays with tumor sections revealed the following: AF-MSCs-endostatin decreased vessel density and cell proliferation; AF-MSCs-sCE2 reduced cell proliferation while it increased apoptosis; and AF-MSCs-endostatin-sCE2 showed a

marked reduction in vessel density and cell proliferation with a dramatic increase in apoptotic cells. Notably, all three GE-AF-MSCs cell lines caused a decrease in the Nestin$^+$ and CD15$^+$ GSC population[32] and an increase in GFAP$^+$ and S100β$^+$ differentiated cells. Together, the simultaneous delivery of endostatin and sCE2 by MSCs in the resection cavity of tumors is the most effective way to repress tumor regrowth in the postsurgery tumor recurrent model.

DISCUSSION

NSCs reside in the subventricular zone in adult brain, providing a specific microenvironment required for the maintenance of their stemness traits.[33] In particular, a perivascular niche in this microenvironment plays a pivotal role in controlling the nature of NSCs.[34] Consistent with NSC biology, GSCs are also localized in the perivascular niche and require this microenvironment for maintaining their cancer stemness.[8] Therefore, disrupting the perivascular niche of GSCs is considered a promising therapeutic modality to completely eradicate GSCs,[8] preventing GSC-driven tumor recurrence after conventional therapy.[35] However, many clinical studies have demonstrated that suppression of tumor angiogenesis in patients with GBM with antiangiogenesis agents such as bevacizumab eventually leads to treatment failure and tumor recurrence,[10] implying that alternative therapeutic approaches are necessary for GBM therapy. Our findings support this clinical limitation of antiangiogenesis strategies, because inhibition of angiogenesis by MSC-mediated delivery of endostatin fails to completely eliminate cancer cells in tumor initiation and postsurgery tumor recurrence models.[36] Moreover, although MSC-mediated delivery of sCE2 in two different glioma models apparently enhanced the antitumor efficacy of CPT11, the overall outcome of these therapeutic approaches could not overcome the current limitation in conventional chemotherapy for GBM patients.[37]

However, the MSC-mediated simultaneous delivery of endostatin and sCE2 in our two glioma models displayed the most outstanding preclinical outcome in repressing either tumor initiation or postsurgery tumor recurrence. In particular, both endostatin and sCE2 appeared to completely suppress tumor initiation through inhibition of angiogenesis and proliferation as well as induction of apoptosis. Additionally, suppression of tumor initiation and regrowth is also attributable to exhausting the pool of GSCs along with an increased differentiated cell population.[38,39]

In conclusion, our study provides a proof of principle for designing a novel therapeutic approach that can eradicate both GSCs and the bulk tumors through disrupting the GSC vascular niche by antiangiogenesis drugs and enhancing the antitumor efficacy of chemotherapeutics by the introduction of a prodrug-activating enzyme.

MATERIALS AND METHODS

Cells and culture conditions. The human glioma cell line U87MG was purchased from the American Type Culture Collection (Manassas, VA), and HUVECs and astrocytes were purchased from Cambrex Bio (Rutherford, NJ). Parental U87MG, ID3-overexpressing U87MG (U87MG-ID3), and EGFRvIII-overexpressing U87MG (U87MG-EGFRvIII) cell lines, as well as astrocytes were maintained in Dulbecco's modified Eagle's medium (Hyclone, Loga, UT) supplemented with 10% fetal bovine serum (Hyclone), 1% penicillin/streptomycin (Gibco, Carlsbad, CA), and 2 mmol/l L-glutamine (Gibco). HUVECs were maintained in endothelial cell basal medium-2 with growth supplements (Clonetics, San Diego, CA). Human AF-derived MSCs (AF-MSCs) were prepared as described previously.[25] Briefly, primary cell cultures of AF were established in α-minimum essential medium (Grand Island, Grand Island, NY) containing 15% embryonic stem cell qualified-fetal bovine serum (Hyclone), 2 mmol/l L-glutamine, and 1% penicillin/streptomycin, supplemented with 18% Chang's medium B and 2% Chang's medium C (Irvine Scientific, Santa Ana, California). At this stage, a mixture of two morphologically distinct groups appears attached and forms colonies. For selective culture of AF-MSCs, cells were harvested by trypsinization and plated in Dulbecco's modified Eagle's medium low glucose medium (Hyclone) supplemented with 10% fetal bovine serum, 1% penicillin/streptomycin, 2 mmol/l L-glutamine, and 4 ng/ml basic fibroblast growth factor (R&D, Minneapolis, MN). A morphologically homogeneous population of AF-MSCs was obtained after two rounds of subculture.

Plasmid construction and gene transfection. The plasmid pSTCF-sCE2, containing a secretable form of human liver carboxylesterase 2 (sCE2) complementary DNA, was kindly provided by Dr Dinja Oosterhoff (VU University Medical Center, Amsterdam, The Netherlands). Human endostatin was cloned into the pSecTag2/HygroB vector (Invitrogen, Carlsbad, CA) as described previously.[40] The resulting plasmid constructs were transfected into U87MG and AF-MSCs using Lipofectamine 2000 (Invitrogen) according to the manufacturer's instructions.

Real-time reverse transcription-PCR. Semiquantitative and real-time reverse transcription-PCR (RT-PCR) were performed to examine mRNA expression levels. Briefly, total RNA was isolated from cells using TRIzol reagent (Invitrogen) according to the manufacturer's instructions. RT was performed using 1 μg of total RNA and MML-V reverse transcriptase (Invitrogen). A 1-μl aliquot of the RT reaction was used to amplify endostatin, carboxylesterase, and GAPDH mRNAs, as well as 18S rRNA using the corresponding gene-specific primer sets. RT-PCR was performed using the iCycler IQ (Bio-Rad) and IQ Supermix with SYBR-Green (Bio-Rad, Hercules, CA). The expression levels of target genes were normalized to 18S rRNA.

In vitro *tube formation assay.* The tube formation assay was performed using an *in vitro* angiogenesis assay kit (Chemicon, Temecula, CA). Briefly, a matrigel-coated plate was prepared by transferring 60 μl of solution admixed with 100 μl of 10× diluent buffer and 900 μl of EC Matrix solution to each well of a precooled 96-well culture plate, and then incubating it at 37 °C for at least 1 hour to allow the matrix solution to coagulate. HUVECs seeded at a density of 1×10^4 cells/well of matrigel-coated plate were cultured in 0.2-μm filtered CM in which 5×10^5 cells of U87MG-hygro, U87MG-endostatin, AF-MSCs-hygro, or AF-MSCs-endostatin cells were cultured in endothelial cell basal medium for 24 hours. After incubation at 37 °C for 18 hours, the tube number of HUVECs in microscopic images (×40 magnification) attained from three random view-fields per well was counted.

In vitro *invasion assay.* The *in vitro* invasive properties of MSCs were examined using the BD Matrigel invasion assay system (BD Biosciences, San Jose, CA). Briefly, basement membrane matrix (BD Biosciences) was diluted to achieve a final protein concentration of 1 mg/ml in serum-free, cold cell culture medium. In total, 100 μl of the diluted matrigel was placed into the upper chamber of a 24-well transwell culture plate (Corning Costar, Corning, NY) and subsequently incubated at 37 °C for at least 4–5 hours for polymerization. MSCs labeled with Cell Staker CSR (Biterials, Seoul, Korea) for 24 hours were harvested with trypsin/EDTA and washed three times with serum-free cell culture medium. CSR-labeled MSCs were resuspended in serum-free medium at a density of 3×10^5 cells/ml, and then 100 μl of the cell suspension was put onto the matrigel-coated upper chamber of transwell culture plate. The

lower chamber of the transwell culture plate was cultured with human astrocytes (NHA), U87MG, U87MG-ID3, or U87MG-EGFRvIII cells. After incubation at 37 °C for 72 hours, transwells were removed from the 24-well plates. CSR-labeled MSCs that invaded into the lower chamber were counted under an inverted fluorescence microscope (Carl Zeiss, Thornwood, NY).

Cytotoxicity assay. Cells were grown in 10% fetal bovine serum-supplemented Dulbecco's modified Eagle's medium with dimethylsulfoxide or CPT11 (10 μmol/l; Sigma, St Louis, MO) for 3 days. In addition, cells were grown in CM obtained from U87MG-control and U87MG-sCE2 cells, as well as from AF-MSCs-hygro and three GE-AF-MSC cell lines with or without CPT11 (5 and 10 μmol/l for U87MG-derived CM, or 10, 20, and 30 μmol/l for AF-MSCs-derived CM) for 3 days. Cell death was determined by flow cytometry after cells were double-stained with Annexin V-fluorescein isothiocyanate (1:100; BD Pharmingen, Sparks, MD) and propidium iodide (50 μg/ml; Sigma). The percentage of dead cells was determined by flow cytometry using the FACS Calibur system and CellQuestPro software (BD Biosciences).

***Subcutaneous and orthotopic cell implantation and imaging* in vivo.** For orthotopic implantation, a mixture of 2.5×10^5 U87MG-EGFRvIII cells labeled with NIR797 dye (Biterials) and 5×10^4 of each genetically engineered AF-MSC line was stereotactically injected into the left striata of nude mice (BALB/c nu/nu; coordinates: anterior-posterior, +2; medial-lateral, +2; dorsal-ventral, −3 mm from the bregma). After 3 days, mice in each group were intravenously injected with 0.5 mg CPT11 (Irinotecan; Hanmi, Seoul, Korea), diluted in 250 μl D5W (5% dextrose) twice a week for a period of 2 weeks. Whole-body fluorescence images of mice were achieved by using an *in vivo* multispectral Maestro II imaging system (CRI) on days 3, 10, and 17 postimplantation. To establish a postsurgery tumor recurrence model using glioma xenografts, 2×10^6 of U87MG-EGFRvIII cells were subcutaneously injected into nude mice (BALB/c nu/nu). When the tumor sizes reached 1.8–2.2 cm^3, ~90% of the tumor mass was surgically removed, and then mice were randomly divided into four groups according to implanted cell types: 2.5×10^5 each of AF-MSCs-hygro, AF-MSCs-endostatin, AF-MSCs-sCE2, or AF-MSCs-endostatin-sCE2 cells admixed with matrigel were implanted in the resection cavity of the tumor. After 3 days, mice in each group were intratumorally injected with 2 μg CPT11 in 100 μl D5W for 7 consecutive days. Tumor sizes were measured 0, 5, 8, 11, and 14 days postsurgical removal of tumors. All mouse experiments were approved by the Animal Care Committee of the College of Life Science and Biotechnology, Korea University, South Korea.

Immunofluorescence and IHC assays. Frozen subcutaneous tumors embedded in optimal cutting temperature medium (Sakura, Kampenhout, Belgium) were cut in serial 10-μm sections for IF assays. Paraffin sections of brains were stained with hematoxylin & eosin for histological evaluation. IHC was performed using a standard technique with the Vectastain Elite ABC kit (Vector, Burlingame, CA). The following antibodies were used for IF and IHC: anti-CD31 (1:200; BD Pharmingen), anti-Ki67 (1:1,000; Novocastra, Newcastle, UK), anti-cleaved caspase 3 (1:200; Cell Signaling, Beverly, MA), anti-Nestin (1:200; Millipore, Billerica, MA), and anti-GFAP (1:100; MP Biomedicals, Solon, OH). Hematoxylin and 4′,6-diamidino-2-phenylindole were used to counterstain IHC and IF sections, respectively. The microvessel density was assessed as described by Leon *et al.*[41] Cell proliferation, the apoptosis index, and the Nestin/$GFAP^+$ cell population revealed by IHC were quantified by counting the number of positively stained cells of 100 nuclei in five randomly chosen high-power fields. Quantitative data achieved from IF assays were analyzed using Image J software (http://rsb.info.nih.gov/ij/). The images of IHC and IF assays were adjusted by Metamorph software (Molecular Devices, Sunnyvale, California).

Statistical analyses. Data were analyzed statistically using two-tailed Student's *t*-test. The level of statistical significance stated in the text was based on the *P* values. $^*P < 0.05$ or $^{**}P < 0.01$ was considered statistically significant.

SUPPLEMENTARY MATERIAL

Figure S1. Representative photos showing *in vitro* tube formation of HUVECs grown in conditional and endothelial cell differentiation medium.

Figure S2. Representative photos showing $CD31^+$ endothelial cells and vessel shapes.

Figure S3. Three genetically engineered AF-MSC cell lines (GE-AF-MSCs) are established by exogenously overexpressing the gene for endostatin, sCE2, or both genes into AF-MSCs.

Figure S4. Molecular and cellular characteristics of three GE-AF-MSC cell lines.

Figure S5. Toxicity and blood chemistry assessment following orthotopically implanted GE-AF-MSCs in normal mouse brain.

Figure S6. Tumor-bearing mice brains were extracted at day 17 postimplantation with a mix of NIR797 dye-labeled U87MG-EGFRvIII and AF-MSCs-hygro or each GE-AF-MSC cell line as indicated.

Figure S7. *In vivo* multispectral imaging of AF-MSCs-sCE2 after labeling of 730 dye and injection into the cavity of 90% surgically resected tumors.

ACKNOWLEDGMENTS

We thank Dr Dinja Oosterhoff (VU University Medical Center, Amsterdam, The Netherlands) for providing the pSTCF-sCE2 plasmid. This work was supported by the Korea Science and Engineering Foundation (KOSEF) NRL Program grant funded by the Korea government (MEST) (No. R0A-2008-000-20024-0) and by the Research Program for New Drug Target Discovery through the National Research Foundation of Korea (NRF) funded by the Ministry of Education, Science and Technology (MEST) (No. 2008–2005234). J.Y., J.-K.K., J.-H.M., S.B. are supported by a graduate fellowship from the Brain Korea 21 project funded by Korea government (MEST). X.J. is supported by a postdoctoral fellowship from the Brain Korea 21 project funded by MEST. S.-H.K. is supported by a postdoctoral fellowship program from NRF funded by MEST (NRF-2009-351-C00137). The authors declared no conflict of interest.

REFERENCES

1. Wen, PY and Kesari, S (2008). Malignant gliomas in adults. *N Engl J Med* **359**: 492–507.
2. Vescovi, AL, Galli, R and Reynolds, BA (2006). Brain tumour stem cells. *Nat Rev Cancer* **6**: 425–436.
3. Singh, SK, Clarke, ID, Terasaki, M, Bonn, VE, Hawkins, C, Squire, J *et al.* (2003). Identification of a cancer stem cell in human brain tumors. *Cancer Res* **63**: 5821–5828.
4. Murat, A, Migliavacca, E, Gorlia, T, Lambiv, WL, Shay, T, Hamou, MF *et al.* (2008). Stem cell-related "self-renewal" signature and high epidermal growth factor receptor expression associated with resistance to concomitant chemoradiotherapy in glioblastoma. *J Clin Oncol* **26**: 3015–3024.
5. Bleau, AM, Hambardzumyan, D, Ozawa, T, Fomchenko, EI, Huse, JT, Brennan, CW *et al.* (2009). PTEN/PI3K/Akt pathway regulates the side population phenotype and ABCG2 activity in glioma tumor stem-like cells. *Cell Stem Cell* **4**: 226–235.
6. Bao, S, Wu, Q, McLendon, RE, Hao, Y, Shi, Q, Hjelmeland, AB *et al.* (2006). Glioma stem cells promote radioresistance by preferential activation of the DNA damage response. *Nature* **444**: 756–760.
7. Al-Hajj, M, Becker, MW, Wicha, M, Weissman, I and Clarke, MF (2004). Therapeutic implications of cancer stem cells. *Curr Opin Genet Dev* **14**: 43–47.
8. Calabrese, C, Poppleton, H, Kocak, M, Hogg, TL, Fuller, C, Hamner, B *et al.* (2007). A perivascular niche for brain tumor stem cells. *Cancer Cell* **11**: 69–82.
9. Moustakas, A and Kreisl, TN (2010). New treatment options in the management of glioblastoma multiforme: a focus on bevacizumab. *Onco Targets Ther* **3**: 27–38.
10. Friedman, HS, Prados, MD, Wen, PY, Mikkelsen, T, Schiff, D, Abrey, LE *et al.* (2009). Bevacizumab alone and in combination with irinotecan in recurrent glioblastoma. *J Clin Oncol* **27**: 4733–4740.
11. Jiang, Y, Jahagirdar, BN, Reinhardt, RL, Schwartz, RE, Keene, CD, Ortiz-Gonzalez, XR *et al.* (2002). Pluripotency of mesenchymal stem cells derived from adult marrow. *Nature* **418**: 41–49.
12. Mareschi, K, Ferrero, I, Rustichelli, D, Aschero, S, Gammaitoni, L, Aglietta, M *et al.* (2006). Expansion of mesenchymal stem cells isolated from pediatric and adult donor bone marrow. *J Cell Biochem* **97**: 744–754.
13. Aboody, KS, Najbauer, J and Danks, MK (2008). Stem and progenitor cell-mediated tumor selective gene therapy. *Gene Ther* **15**: 739–752.

14. Colter, DC, Class, R, DiGirolamo, CM and Prockop, DJ (2000). Rapid expansion of recycling stem cells in cultures of plastic-adherent cells from human bone marrow. *Proc Natl Acad Sci USA* **97**: 3213–3218.
15. Conget, PA and Minguell, JJ (2000). Adenoviral-mediated gene transfer into ex vivo expanded human bone marrow mesenchymal progenitor cells. *Exp Hematol* **28**: 382–390.
16. Nakamizo, A, Marini, F, Amano, T, Khan, A, Studeny, M, Gumin, J *et al.* (2005). Human bone marrow-derived mesenchymal stem cells in the treatment of gliomas. *Cancer Res* **65**: 3307–3318.
17. Hamada, H, Kobune, M, Nakamura, K, Kawano, Y, Kato, K, Honmou, O *et al.* (2005). Mesenchymal stem cells (MSC) as therapeutic cytoreagents for gene therapy. *Cancer Sci* **96**: 149–156.
18. Sasportas, LS, Kasmieh, R, Wakimoto, H, Hingtgen, S, van de Water, JA, Mohapatra, G *et al.* (2009). Assessment of therapeutic efficacy and fate of engineered human mesenchymal stem cells for cancer therapy. *Proc Natl Acad Sci USA* **106**: 4822–4827.
19. O'Reilly, MS, Boehm, T, Shing, Y, Fukai, N, Vasios, G, Lane, WS *et al.* (1997). Endostatin: an endogenous inhibitor of angiogenesis and tumor growth. *Cell* **88**: 277–285.
20. Dhanabal, M, Ramchandran, R, Volk, R, Stillman, IE, Lombardo, M, Iruela-Arispe, ML *et al.* (1999). Endostatin: yeast production, mutants, and antitumor effect in renal cell carcinoma. *Cancer Res* **59**: 189–197.
21. Satoh, T, Hosokawa, M, Atsumi, R, Suzuki, W, Hakusui, H and Nagai, E (1994). Metabolic activation of CPT-11, 7-ethyl-10-[4-(1-piperidino)-1- piperidino] carbonyloxycamptothecin, a novel antitumor agent, by carboxylesterase. *Biol Pharm Bull* **17**: 662–664.
22. Gupta, E, Mick, R, Ramirez, J, Wang, X, Lestingi, TM, Vokes, EE *et al.* (1997). Pharmacokinetic and pharmacodynamic evaluation of the topoisomerase inhibitor irinotecan in cancer patients. *J Clin Oncol* **15**: 1502–1510.
23. Negoro, S, Fukuoka, M, Masuda, N, Takada, M, Kusunoki, Y, Matsui, K *et al.* (1991). Phase I study of weekly intravenous infusions of CPT-11, a new derivative of camptothecin, in the treatment of advanced non-small-cell lung cancer. *J Natl Cancer Inst* **83**: 1164–1168.
24. Oosterhoff, D, Witlox, MA, van Beusechem, VW, Haisma, HJ, Schaap, GR, Bras, J *et al.* (2003). Gene-directed enzyme prodrug therapy for osteosarcoma: sensitization to CPT-11 *in vitro* and *in vivo* by adenoviral delivery of a gene encoding secreted carboxylesterase-2. *Mol Cancer Ther* **2**: 765–771.
25. Yoon, BS, Moon, JH, Jun, EK, Kim, J, Maeng, I, Kim, JS *et al.* (2010). Secretory profiles and wound healing effects of human amniotic fluid-derived mesenchymal stem cells. *Stem Cells Dev* **19**: 887–902.
26. Joki, T, Machluf, M, Atala, A, Zhu, J, Seyfried, NT, Dunn, IF *et al.* (2001). Continuous release of endostatin from microencapsulated engineered cells for tumor therapy. *Nat Biotechnol* **19**: 35–39.
27. Sugawa, N, Ekstrand, AJ, James, CD and Collins, VP (1990). Identical splicing of aberrant epidermal growth factor receptor transcripts from amplified rearranged genes in human glioblastomas. *Proc Natl Acad Sci USA* **87**: 8602–8606.
28. Reyes, M and Verfaillie, CM (2001). Characterization of multipotent adult progenitor cells, a subpopulation of mesenchymal stem cells. *Ann N Y Acad Sci* **938**: 231–233; discussion 233.
29. Xu, W, Zhang, X, Qian, H, Zhu, W, Sun, X, Hu, J *et al.* (2004). Mesenchymal stem cells from adult human bone marrow differentiate into a cardiomyocyte phenotype *in vitro*. *Exp Biol Med (Maywood)* **229**: 623–631.
30. Inda, MM, Bonavia, R, Mukasa, A, Narita, Y, Sah, DW, Vandenberg, S *et al.* (2010). Tumor heterogeneity is an active process maintained by a mutant EGFR-induced cytokine circuit in glioblastoma. *Genes Dev* **24**: 1731–1745.
31. Williams, J, Lansdown, R, Sweitzer, R, Romanowski, M, LaBell, R, Ramaswami, R *et al.* (2003). Nanoparticle drug delivery system for intravenous delivery of topoisomerase inhibitors. *J Control Release* **91**: 167–172.
32. Son, MJ, Woolard, K, Nam, DH, Lee, J and Fine, HA (2009). SSEA-1 is an enrichment marker for tumor-initiating cells in human glioblastoma. *Cell Stem Cell* **4**: 440–452.
33. Sirko, S, von Holst, A, Wizenmann, A, Götz, M and Faissner, A (2007). Chondroitin sulfate glycosaminoglycans control proliferation, radial glia cell differentiation and neurogenesis in neural stem/progenitor cells. *Development* **134**: 2727–2738.
34. Ramírez-Castillejo, C, Sánchez-Sánchez, F, Andreu-Agulló, C, Ferrón, SR, Aroca-Aguilar, JD, Sánchez, P *et al.* (2006). Pigment epithelium-derived factor is a niche signal for neural stem cell renewal. *Nat Neurosci* **9**: 331–339.
35. Bar, EE, Chaudhry, A, Lin, A, Fan, X, Schreck, K, Matsui, W *et al.* (2007). Cyclopamine-mediated hedgehog pathway inhibition depletes stem-like cancer cells in glioblastoma. *Stem Cells* **25**: 2524–2533.
36. Liu, F, Tan, G, Li, J, Dong, X, Krissansen, GW and Sun, X (2007). Gene transfer of endostatin enhances the efficacy of doxorubicin to suppress human hepatocellular carcinomas in mice. *Cancer Sci* **98**: 1381–1387.
37. Minniti, G, Muni, R, Lanzetta, G, Marchetti, P and Enrici, RM (2009). Chemotherapy for glioblastoma: current treatment and future perspectives for cytotoxic and targeted agents. *Anticancer Res* **29**: 5171–5184.
38. Beug, H (2009). Breast cancer stem cells: eradication by differentiation therapy? *Cell* **138**: 623–625.
39. Massard, C, Deutsch, E and Soria, JC (2006). Tumour stem cell-targeted treatment: elimination or differentiation. *Ann Oncol* **17**: 1620–1624.
40. Yoon, SS, Eto, H, Lin, CM, Nakamura, H, Pawlik, TM, Song, SU *et al.* (1999). Mouse endostatin inhibits the formation of lung and liver metastases. *Cancer Res* **59**: 6251–6256.
41. Leon, SP, Folkerth, RD and Black, PM (1996). Microvessel density is a prognostic indicator for patients with astroglial brain tumors. *Cancer* **77**: 362–372.